EUROPHYSICS LETTERS 1 April 2004

Europhys. Lett., **66** (1), pp. 125–131 (2004)
DOI: 10.1209/epl/i2003-10140-1

Sedimentation and multi-phase equilibria in mixtures of platelets and ideal polymer

H. H. Wensink and H. N. W. Lekkerkerker(*)
Van 't Hoff Laboratory for Physical and Colloid Chemistry, Debye Institute Utrecht University - Padualaan 8, 3584 CH Utrecht, The Netherlands

(received 19 November 2003; accepted in final form 26 January 2004)

PACS. 82.70.Dd – Colloids.
PACS. 64.70.Md – Transitions in liquid crystals.

Abstract. – The role of gravity in the phase behaviour of mixtures of hard colloidal plates without and with non-adsorbing ideal polymer is explored theoretically. By analyzing the (macroscopic) osmotic equilibrium conditions, we show that sedimentation of the colloidal platelets is significant on a height range of even a centimeter. Gravity enables the system to explore a large density range within the height of a test tube which may give rise to the simultaneous presence of multiple phases. As to plate-polymer mixtures, it is shown that sedimentation may lead to a four-phase equilibrium involving an isotropic gas and liquid phase, nematic and columnar phase. The phenomenon has been observed experimentally in systems of colloidal gibbsite platelets mixed with PDMS polymer.

It is well known that adding non-adsorbing polymer to a colloidal dispersion induces an attractive depletion potential of mean force between the colloidal particles [1–3]. For colloidal spheres, the attractive potential has been shown to give rise to a phase separation in a colloid-poor "gas" and colloid-rich "liquid" or "solid" phase at sufficiently high concentrations of the colloid and the polymer [4–8]. Compared to colloidal spheres, the behaviour of dispersions of rod- and plate-like colloids mixed with polymer is richer due to their possibility to form liquid-crystal phases, *i.e.* nematic (N), smectic (Sm) and columnar (C). Recent experiments on mixtures of colloidal gibbsite platelets and non-adsorbing polymer [9] have uncovered the phase behavior of plate-polymer mixtures. A manifestation of the rich phase behaviour of these mixtures is the observation of a four-phase equilibrium involving both isotropic gas and liquid phases along with nematic and columnar states. The appearance of multiple phases seems to conflict with the phase rule of Gibbs which states that the number of coexisting phases is limited to three for an athermal binary mixture. One of the possible explanations conjectured by the authors [9] is that the observation might be due to the polydispersity in particle size. The presence of many components (*i.e.* platelets with different diameters and thicknesses) in principle allows for a coexistence of arbitrarily many phases.

Another possibility to reconcile the experimental results with Gibbs' phase rule is by accounting for an external gravitational field. Sedimentation of particles leads to a density

(*) E-mail: h.n.w.lekkerkerker@chem.uu.nl

gradient which facilitates the formation of multiple phases in a vessel of sufficient height. In this paper we scrutinize the effect of sedimentation in systems of colloidal platelets with and without added polymer from a simple osmotic compression treatment. We will first consider a one-component system of colloidal platelets and then study the influence of the polymer-induced depletion attraction using a mean-field free-volume theory [10].

Sedimentation equilibrium: one-component system. – Let us consider a vessel containing colloidal particles (platelets) in osmotic equilibrium with a dispersing solvent with a chemical potential μ_0 subject to a gravitational field along the z-direction of the vessel. We assume that the concentration profile of the colloids is sufficiently smooth so that the system is *locally* in a homogeneous equilibrium state between z and $z + \mathrm{d}z$. This is usually the case if the particles are not too large and heavy and if the dispersion is not too close to a critical point. The (macroscopic) condition for sedimentation equilibrium reads

$$-\left(\frac{\partial \Pi}{\partial \rho}\right)_{T,\mu_0} \frac{\mathrm{d}\rho}{\mathrm{d}z} = m^* g \rho \tag{1}$$

in terms of the osmotic compressibility $(\partial\rho/\partial\Pi)_{T,\mu_0}$ of the dispersion and the buoyant mass m^* of the colloidal particle (g is the gravitational acceleration). The concentration profile $\rho(z)$ of the colloids can be obtained from eq. (1) if the osmotic pressure as a function of ρ, *i.e.* the equation of state (EOS), is known.

In the present study we will encounter phase-separated samples containing a number of distinct phases. Since these phases are generally described by *different* equations of state, it is convenient to treat each daughter phase i separately and assign a phase height H_i to each of them. Recasting eq. (1) in dimensionless form by introducing the height parameter $\zeta = z/H_{(i)}$ (with $0 < \zeta < 1$) and dimensionless plate concentration $c_i = \rho_i D^3$ (with D the plate diameter) corresponding to phase i yields

$$-\frac{1}{c_i(\zeta)} \frac{\mathrm{d}c_i(\zeta)}{\mathrm{d}\zeta} \left(\frac{\partial\big(\beta \Pi_i D^3\big)}{\partial c_i(\zeta)}\right)_{T,\mu_0} = \tilde{H}_i \tag{2}$$

with $\beta = 1/k_\mathrm{B}T$ and $\tilde{H}_i = H_i/\xi$ the height of phase i rendered dimensionless by relating it to the *gravitational length* $\xi = k_\mathrm{B}T/m^*g$ which is on the order of $10^{-3}\,\mathrm{m}$ for the colloidal dispersions of gibbsite platelets we consider in this paper. The average concentration $c_{0,i}$ in phase i follows from

$$\int_0^1 c_i(\zeta)\mathrm{d}\zeta = \int_{c_{\mathrm{b},i}}^{c_{\mathrm{t},i}} c_i'(\zeta)\frac{\mathrm{d}\zeta}{\mathrm{d}c_i'} dc_i' = c_{0,i}\,, \tag{3}$$

where $c_{\mathrm{t},i}$ and $c_{\mathrm{b},i}$ denote the concentrations at the top and the bottom of the phase, respectively. The average concentration c_0 of the *sample* then follows from a simple linear combination $c_0 = \sum_i c_{0,i}\tilde{H}_i/\tilde{H}$ with $\tilde{H} = \sum_i \tilde{H}_i$ the dimensionless sample height.

Note that in an experimental situation these concentrations are to be determined from a *given* average sample concentration c_0. In order to solve eq. (2) for colloidal platelets, we must know the EOS $\Pi_i(c_i)$ for the different liquid-crystal states (*viz.* isotropic (I), nematic (N) and columnar (C)) encountered upon densifying these systems. As a quantitative input we use fits to the EOS obtained from Monte Carlo simulations of hard platelets performed by Zhang *et al.* [11]. A polynomial of the K-th order was used as a fitting function so that $\beta\Pi_i D^3 = \sum_{n=1}^{K} a_{n,i} c_i^n$, with i = I, N, C. The coefficients $a_{n,i}$ pertaining to state i can be found in ref. [11]. The polynomial form of the EOS allows for a simple analytic solution of the concentration profile from eq. (2) in the different phases.

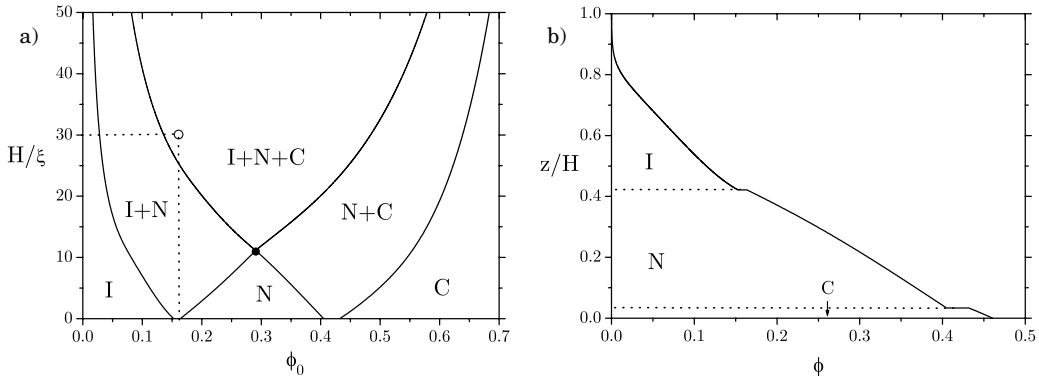

Fig. 1 – a) Phase diagram for colloidal platelets with $L/D = 0.05$ in a gravitational field. Plotted is the reduced *sample* height $\tilde{H} = H/\xi$ *vs.* the overall plate volume fraction ϕ_0. The three-phase region opens up at $H = 11.15\xi$. b) Concentration profile of a sample with overall volume fraction $\phi_0 = 0.157$ and vessel height $H = 30\xi$ (corresponding to the open dot in a). Plotted is the relative height z/H *vs.* ϕ. The I-N and N-C phase boundaries are indicated by the horizontal dotted lines.

The effect of gravity on the phase behaviour of the colloidal platelets is presented in fig. 1. The curves represent so-called *cloud curves* which indicate the minimum sample height (and associated overall volume fraction) needed to induce the formation of an infinitesimal amount of a new phase at the top and/or the bottom of the vessel due to sedimentation of the particles. On the horizontal axis we find the coexistence densities for the I-N and N-C transitions at zero gravity, which would correspond to a vessel with potentially zero height. Figure 1a) shows that a vessel height of about 10 gravitational lengths already leads to significant changes in the phase diagram. A large three-phase isotropic-nematic-columnar region is encountered which opens up at the state point indicated by the black dot. At the associated volume fraction ($\phi_0 = 0.291$) the system is fully nematic at short sample heights but as soon as the height exceeds 11.15 gravitational lengths, two additional fractions of an isotropic and columnar phase are split off *simultaneously* at the top and bottom of the sample, respectively. To compare with actual sample heights we use the following expression for the gravitation length, $\xi = k_{\rm B}T/(g v_{\rm plate}\rho^*_{\rm plate})$ with $v_{\rm plate} = \frac{\pi}{4}LD^2$ the colloid volume. Using experimental data for the colloidal gibbsite platelets dispersed in toluene (plate dimensions $D = 180\,\mathrm{nm}$, $L = 12\,\mathrm{nm}$ and buoyant density $\rho^*_{\rm plate} = 1.5\ 10^3\,\mathrm{kg/m^3}$) we obtain $\xi = 0.9\,\mathrm{mm}$. This means that the three-phase isotropic-nematic-columnar equilibria in fig. 1 may be expected in samples larger than a centimeter, which is comparable to the typical height of a test tube. Figure 1b) shows an example of a concentration profile one may encounter experimentally in a sample with overall plate volume fraction of 15.7% and height of 2.7 cm. The scenario is that the system initially phase-separates into equal portions of an isotropic and nematic phase. At a later stage, a columnar fraction will be formed at the bottom of the vessel due to slow sedimentation of the platelets. At sedimentation equilibrium, the I, N and C phases, respectively, occupy 58, 39 and 3% of the system volume.

Plate-polymer mixtures. – We now turn to systems of colloidal platelets (component "1") mixed with non-adsorbing ideal polymers (denoted by "p") in a solvent. The gravitational length of the polymer is much larger than that of the colloidal particles ($\xi_{\rm p} \gg \xi_1$) due to its negligible buoyant mass. We may therefore assume that there is no external force acting on the polymer coils and that the chemical potential of the polymer can be considered *constant* throughout the system. The mixture can thus be treated as an *effective* one-component

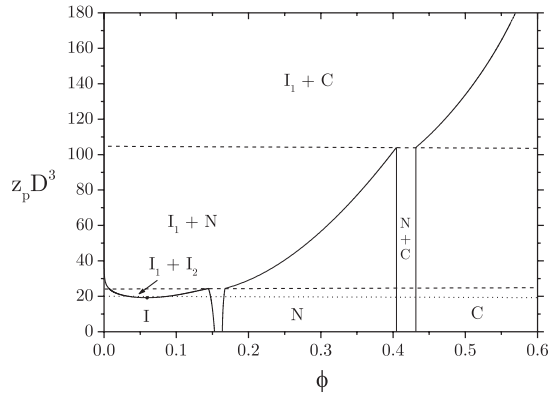

Fig. 2 – Phase diagram of a plate-polymer mixture with $L/D = 0.05$ and $q = 0.355$ in the fugacity-volume fraction plane, reproduced from ref. [11]. On the vertical axis, the region of stable isotropic gas-liquid (I_1-I_2) equilibria is confined between a lower critical point at $z_pD^3 = 19.233$ (dotted line) and the I_1-I_2-N triple line at $z_pD^3 = 24.454$ (lower dashed line). The upper dashed line at $z_pD^3 = 104$ represents the I_1-N-C triple line.

system of colloidal platelets in a gravitational field and the osmotic pressure balance now reads, analogously to eq. (1),

$$-\left(\frac{\partial \Pi}{\partial \rho_1}\right)_{T,\mu_0,\mu_p} \frac{\mathrm{d}\rho_1}{\mathrm{d}z} = m_1^* g \rho_1 \,, \tag{4}$$

at constant μ_p. Similar to eq. (2), we can rewrite this equilibrium condition in dimensionless form. Substituting the EOS for a colloid-polymer mixture from a free-volume treatment of the Asakura-Osawa model (see the appendix) yields the following differential equation describing the colloid density profile $c_{1,i}(\zeta)$ in the daughter phase i:

$$-\frac{1}{c_{1,i}(\zeta)} \frac{\mathrm{d}c_{1,i}(\zeta)}{\mathrm{d}\zeta} \left[\left(\frac{\partial \left(\beta \Pi_i^{(0)} D^3\right)}{\partial c_{1,i}} \right)_{T,\mu_0,\mu_2} - z_p D^3 \left(\frac{\mathrm{d}^2 \alpha_i}{\mathrm{d}c_{1,i}^2} \right) c_{1,i}(\zeta) \right] = \tilde{H}_i \tag{5}$$

which must be solved along with the auxiliary condition for the overall concentration, eq. (3). Comparing with eq. (2), we see that the terms between square brackets now represent an *effective* (inverse) osmotic compressibility. The first contribution is the inverse compressibility of the one-component plate system, whereas the second term accounts for the effective depletion attraction between the platelets due to the presence of the polymer. The strength of the depletion attraction can be varied by changing the fugacity z_p of the polymer, related to the chemical potential via $z_p = \exp[\beta \mu_p]/V$. Note that the result for a one-component system (eq. (2)) is recovered for $z_p = 0$, as it should. The effective compressibility also depends on the fraction of *free volume* α_i available to the polymer in the liquid-crystal state i. Explicit expressions for α_i are given in the appendix. It is easily verified that $\mathrm{d}^2\alpha_i/\mathrm{d}c_{1,i}^2$ is generally positive for all states i = I, N, C, implying that the effective osmotic compressibility is *larger* than that of a pure system of plates due to the attractive depletion forces, as we intuitively expect.

In fig. 2 we have depicted a phase diagram for the zero-gravity case reproduced from ref. [11]. The values for the plate aspect-ratio and the polymer-to-plate size ratio $q = 2R_g/D$ (with R_g the polymer radius of gyration) are chosen such as to match the experimental values for the gibbsite-PDMS mixtures studied by Van der Kooij *et al.* [9]. The volume fractions in the

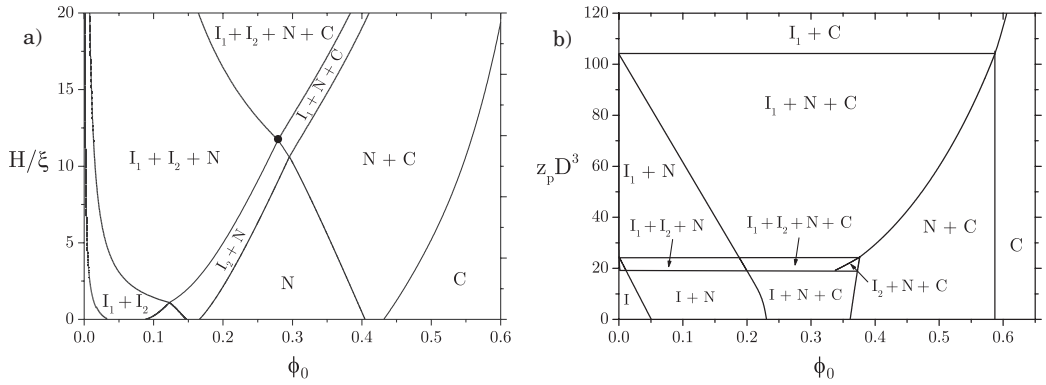

Fig. 3 – a) Phase diagram of the same mixture as in fig. 2 in a gravitational field at (constant) fugacity $z_{\rm p}D^3 = 20$. Plotted is the relative sample height $\tilde{H} = H/\xi$ *vs.* the overall plate volume fraction. The four-phase region opens up at $H = 11.70\xi$ (black dot). b) Same diagram in a reservoir fugacity-volume fraction representation at fixed vessel height $H = 1.5\,\mathrm{cm}$ ($H/\xi = 16.67$).

coexisting phases can be deduced from tie lines given by horizontal lines in this representation. At low reservoir fugacity the phase behaviour of the mixture differs only marginally from that of the pure system. At $z_{\rm p}D^3 > 19.233$, the isotropic phase becomes unstable with respect to a demixing into an isotropic gas phase (I_1) and a liquid phase (I_2). The gas phase is poor in colloid but rich in polymer, vice versa for the liquid phase. The nematic-columnar transition is unaffected by the presence of the polymer up to the I_1-N-C triple line located at $z_{\rm p}D^3 = 104$. At higher fugacities the depletion attraction is strong enough to induce a transition from an isotropic gas (I_1) to a columnar solid (C) phase, without the intervention of a nematic phase.

In fig. 3a) we have depicted a phase representation, analogous to fig. 1, of the same mixture in a gravitational field at fixed reservoir fugacity $z_{\rm p}D^3 = 20$. Also here, we see that sedimentation leads to remarkably rich phase behaviour; several multi-phase equilibria appear that are not present in the zero-gravity case in fig. 2. Most notably, a four-phase region opens up at $H/\xi = 11.70$ which, recalling that $\xi = 0.9\,\mathrm{mm}$, is again about a centimeter. An equilibrium involving isotropic gas, liquid, nematic and columnar phases has been observed in the gibbsite-PDMS mixtures [9]. We stress that the experimental observation of four distinct phases in a tube of a few centimeters is related in a fortuitous way to the platelets' size (and hence their gravitational length). If the platelets had been much larger, they would rather have formed a dense, quasi-uniform sediment at the bottom of the tube. If they were much smaller, gravity may not have been strong enough to enforce a four-phase sedimentation equilibrium.

From an experimental standpoint it is more appropriate to fix the total sample height rather than the reservoir fugacity. In fig. 3b) we show a representation in terms of the fugacity *vs.* the overall volume fraction at fixed sample height $H = 1.5\,\mathrm{cm}$, which is the typical length of the test tubes used in experiment [9]. Unlike fig. 2, this representation does *not* provide information about the composition of the phases present, it merely indicates which phases can be expected in a sample with a fixed height and a given overall density and reservoir fugacity. Comparing with fig. 2, we see that the four-phase region in fig. 3b) must be confined within the range $19.233 < z_{\rm p}D^3 < 24.454$ since only there both stable I_1-I_2 and N-C two-phase equilibria occur at low and high densities, respectively.

We can therefore conclude that gravity enables the colloidal platelets to scan a large density range within the range of a few centimeters. Since mixtures of plates and ideal polymer display a number of phase transitions within a relatively small range of concentrations, sedimentation

may thus lead to the presence of multiple phases in a test tube. It is important to note that the *maximum* number of phases that can appear simultaneously in the tube is governed solely by the effective interactions between the colloids. In the present system these interactions are tuned directly by the polymer chemical potential in the reservoir. Gravity can therefore only induce the formation of those phases that are allowed at a particular interaction strength, as becomes evident from comparing fig. 3b) to fig. 2.

Final remarks. – The theoretical results obtained thus far prompt us to reconsider observations in other colloidal mixtures. For instance, mixtures of hard rod- with plate-like colloids also display rich phase behaviour with a possibility of multi-phase equilibria involving up to five phases [12]. The five-phase equilibrium comprises (from top to bottom) an isotropic, rod-rich nematic (N^+), X-phase (its symmetry has not been identified yet), plate-rich nematic (N^-) and a columnar phase. Also in these mixtures, the polydispersity in particle size (*i.e.* both plate-diameter and rod-length) is appreciable. Although the phase behaviour is certainly influenced by polydispersity, the effect of gravity should not be neglected. Given the present results, one may question to what extent these multi-phase equilibria are induced by an external gravitational field acting on the particles. This issue will be deferred to future investigation. However, we can already point out that in these mixtures both components will generally be subject to the gravitational field so that the effective one-component approach, described in this paper, cannot be applied for binary mixtures of colloids. Consequently, the chemical potentials of the species are coupled and therefore cannot be varied independently (as we could do for $\mu_{\rm p}$ in this study) [13]. Clearly, the coupling leads to more complicated equilibrium conditions than the ones shown here.

Appendix

Free-volume theory. – The semi-grand canonical potential for a mixture of colloids and ideal polymer within a mean-field free-volume treatment of the Asakura-Oosawa model [10,11] is given by

$$\beta\Omega\big(N,V,T,\mu_0,z_{\rm p}\big) = \beta F^{(0)}\big(N,V,T,\mu_0,z_{\rm p}=0\big) - z_{\rm p}\alpha V \tag{6}$$

with $\beta = 1/k_{\rm B}T$. Here, N is the number of colloidal particles in the system and $F^{(0)}$ is the reference (Helmholtz) free energy of the unperturbed colloidal system. Furthermore, $z_{\rm p}$ is the fugacity of the polymer in a reservoir, separated from the system by a semi-permeable membrane which only allows for exchange of polymer and solvent. Note that for ideal polymers, $z_{\rm p}$ is simply equal to the polymer concentration $\rho_{\rm p} = N_{\rm p}/V$. Finally, α represents the free-volume fraction averaged over all colloidal configurations of the *unperturbed* system. As such α depends only upon the colloid density $\rho = N/V$ in the system. The osmotic pressure of the colloid-polymer mixture follows from eq. (6) using the standard derivative $\Pi = -(\partial\Omega/\partial V)_{N,T,\mu_{\rm p}}$:

$$\tilde{\Pi} = \tilde{\Pi}^{(0)} + z_{\rm p}D^3\left[\alpha - \rho\frac{{\rm d}\alpha}{{\rm d}\rho}\right] \tag{7}$$

in terms of the dimensionless pressure $\tilde{\Pi}^{(0)} \equiv \beta\Pi^{(0)}D^3$ of the reference plate system. An expression for the free-volume fraction α can be obtained from scaled particle theory [14,15]. Zhang *et al.* [16] derived expressions for *cut spheres* with diameter D and thickness L. Cut spheres are plate-like objects obtained by slicing two caps off a sphere of diameter D, at two planes parallel to the equatorial plane with equal distance $L/2$. The general expression for the free volume reads

$$\alpha = (1-\phi)\exp\big[-\big(Ay + By^2 + C\tilde{\Pi}^{(0)}\big)\big] \tag{8}$$

with $y \equiv \phi/(1-\phi)$ and ϕ the plate volume fraction. The expression still depends on the pressure $\Pi^{(0)}$ of the reference cut sphere system, for which no analytical expression is available yet. Specific expressions α_i for the different liquid-crystal states i can be obtained by inserting the corresponding EOS $\tilde{\Pi}_i^{(0)}$ from the simulation fits. The coefficients are given by

$$\begin{aligned} A &= \frac{q\big(1+2l-l^2\big)+q^2\big[2l+\big(\frac{\pi}{2}-\arcsin l\big)\big]\sqrt{1-l^2}}{\big(l-l^3/3\big)}\,, \\ B &= \frac{q^2\big(1+2l-l^2\big)^2}{2\big(l-l^3/3\big)^2}\,, \qquad C=\pi q^3/6 \end{aligned} \tag{9}$$

with $l = L/D$ the aspect ratio and $q = 2R_{\rm g}/D$ the size ratio of the ideal polymer coil and the platelet. The volume fraction follows from $\phi = (\pi/4)\rho D^3(l - l^3/3)$.

* * *

We thank G. J. Vroege and M. Oversteegen for a critical reading of the manuscript.

REFERENCES

[1] Asakura S. and Oosawa F., *J. Chem. Phys.*, **22** (1954) 1255.
[2] Asakura S. and Oosawa F., *J. Polym. Sci.*, **33** (1958) 183.
[3] Vrij A., *Pure Appl. Chem.*, **48** (1976) 471.
[4] Vester C. F., *Kolloid-Z.*, **84** (1938) 63.
[5] de Hek H. and Vrij A., *J. Colloid Interface Sci.*, **84** (1981) 409.
[6] Vincent B., Edwards J., Emmet S. and Groot R. D., *Colloids Surf.*, **31** (1988) 267.
[7] Gast A. P., Russel W. B. and Hall C. K., *J. Colloid Interface Sci.*, **109** (1986) 161.
[8] Illet S. M., Orrock A., Poon W. C. K. and Pusey P. N., *Phys. Rev. E*, **51** (1995) 1344.
[9] van der Kooij F. M., Vogel M. and Lekkerkerker H. N. W., *Phys. Rev. E*, **62** (2000) 5397.
[10] Lekkerkerker H. N. W., Poon W. C. K., Pusey P. N., Stroobants A. and Warren P. B., *Europhys. Lett.*, **20** (1992) 559.
[11] Zhang S. D., Reynolds P. A. and van Duijneveldt J. S., *J. Chem. Phys.*, **117** (2002) 9947.
[12] van der Kooij F. M. and Lekkerkerker H. N. W., *Langmuir*, **16** (2000) 10144.
[13] Vrij A., *J. Chem. Phys.*, **72** (1980) 3735.
[14] Reiss H., Frisch H. L. and Lebowitz J. L., *J. Chem. Phys.*, **31** (1959) 369.
[15] Lebowitz J. L., Helfand E. and Praestgaard E., *J. Chem. Phys.*, **43** (1965) 774.
[16] Zhang S. D., van Duijneveldt J. S. and Reynolds P. A., *Mol. Phys.*, **100** (2002) 3041.